Published in final edited form as:

Anal Chem. 2018 April 03; 90(7): 4657–4662. doi:10.1021/acs.analchem.7b05200.

Negative selection by spiral inertial microfluidics improves viral recovery and sequencing from blood

Kyungyong Choi[1,2], **Hyunryul Ryu**[1], **Katherine J Siddle**[3,4], **Anne Piantadosi**[3,5], **Lisa Freimark**[3], **Daniel J Park**[3], **Pardis Sabeti**[3,4,6,7], and **Jongyoon Han**[1,2,8]

[1]Research Laboratory of Electronics

[2]Department of Electrical Engineering and Computer Science, Massachusetts Institute of Technology, 77 Massachusetts Avenue, Cambridge, MA 02139, USA

[3]Broad Institute of MIT and Harvard, 75 Ames Street, Cambridge, MA 02142, USA

[4]Center for Systems Biology, Department of Organismic and Evolutionary Biology, Harvard University, Cambridge, MA, 02138, USA

[5]Division of Infectious Disease, Department of Medicine, Massachusetts General Hospital, Boston, MA, 02114

[6]Department of Immunology and Infectious Disease, Harvard School of Public Health, Boston

[7]Howard Hughes Medical Institute, Chevy Chase, Maryland, USA

[8]Department of Biological Engineering, Massachusetts Institute of Technology, 77 Massachusetts Avenue, Cambridge, MA 02139, USA

Abstract

In blood samples from patients with viral infection, it is often important to separate viral particles from human cells, for example to minimize background in performing viral whole genome sequencing. Here, we present a microfluidic device that uses spiral inertial microfluidics with continuous circulation to separate host cells from viral particles and free nucleic acid. We demonstrate that this device effectively reduces white blood cells, red blood cells, and platelets from both whole blood and plasma samples with excellent recovery of viral nucleic acid. Furthermore, microfluidic separation leads to greater viral genome coverage and depth, highlighting an important application of this device in processing clinical samples for viral genome sequencing.

Graphical Abstract

Corresponding Authors Jongyoon Han (jyhan@mit.edu, Tel: 617-253-2290).

Supporting Information

Supplementary figure (Manuscript_supporting information.pdf)

Conflict of Interest Disclosure

The authors have filed a patent application on the technology described here.

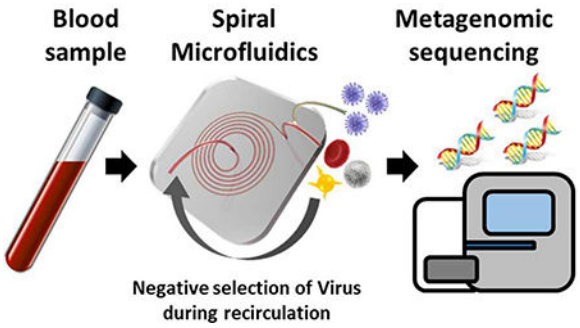

Introduction

Isolation of viral nucleic acid from human clinical samples is important in the diagnosis of many infectious diseases and also represents the critical first step in scientific studies of viral genomics and pathogenesis. Recently, metagenomic sequencing has become a prominent method for virus detection[1,2], discovery[3–6], and viral genome sequencing for studies of evolution and pathogenesis[7,8]. In this technique, all DNA, RNA, or total nucleic acid in a sample is sequenced in an unbiased fashion, and computational algorithms are used to recover the viral sequencing reads of interest. The major advantage of this technique is that it is a flexible methodology that can be applied to any virus, including settings in which the pathogen may be unknown or novel. However, a substantial limitation is the recovery of sequencing reads from the human host, which vastly outnumber viral sequencing reads even in low-cell-content fluids like plasma and cerebrospinal fluid. This leads to costly high-depth sequencing and limits the recovery of reads from low abundance viruses. This has prompted the development of host-depletion methods such as selective removal of human ribosomal RNA[9,10], however this is less useful in detecting and sequencing DNA viruses where background from host DNA remains.

Microfluidic isolation of viral particles and free nucleic acid offers an opportunity to enhance detection of both RNA viruses and DNA viruses, and importantly can be performed directly from whole blood, eliminating the need for centrifugation and perhaps enhancing the detection of some viruses (*e.g.* West Nile Virus) that adhere to red blood cells[11,12]. Earlier microfluidic devices implemented capillary imbibition[13,14], blood cell sedimentation[15,16], cross-flow filtration[17–19], on-chip centrifugation[20,21], and membrane-based filtration[22,23]. These various applications were limited by non-continuous operation, low throughput, or small sample volume, and clogging and fouling of filter/membrane. Shim *et al.*[13] and Lee *et al.*[14] developed micro-channel structures that are either packed or coated with micro/nanosized silica beads to induce a capillary plasma extraction from whole blood. Dimov *et al.*[16] demonstrated a self-powered integrated microfluidic platform in which plasma is separated by natural sedimentation inside the microfluidic channel while the sample transport is propelled by the self-contained vacuum in the channel. VanDelinder *et al.*[18] devised a microfluidic device which can separate plasma from diluted whole blood by size exclusion in a cross-flow. Haeberle *et al.*[20] presented a centrifugation-based microfluidic device on a disc which enables plasma extraction from whole blood by carefully manipulating centrifugal force to transport the blood as well as to sediment the

cellular pellet and to decant the plasma inside the device structure. Researchers have adopted membrane-based microfluidic devices to extract plasma from whole blood samples spiked with viruses or drawn from virus-infected patients and successfully recovered sufficient virus to be quantified with a viral load test.[22,23] Wang *et al.*[23] fabricated a filter-based lab-on-a-chip device which can isolate plasma as well as viruses from unprocessed whole blood and reported viral recovery of 73–83%. Liu *et al.*[22] also demonstrated a membrane-based plasma separating device which is facilitated by gravitational sedimentation and were able to recover 82–96% of HIV virus from multiple load samples. Recently, inertial microfluidics which can separate particles based on their sizes by utilizing and balancing forces inside the micro-channel have been spotlighted as an alternative to prepare biological samples in a continuous, high-throughput, non-clogging manner before further downstream assays.[24–31] Rafeie *et al.*[30] presented a high-throughput slanted spiral microchannel device that can extract plasma from diluted whole blood from small to large volume (1–100mL) with a maximum processing flow rate of 24 mL/min. However, performance of inertial microfluidics is often limited by conventional single-pass operation which results in an intrinsic trade-off between purity and recovery when the window of optimal operation is narrow.

As an effort to remedy this issue of single-pass operation, our group introduced a closed-loop operation of spiral microfluidic device, called “C-sep”, where both enrichment and recovery of target cells can be maximized by continuously feeding the inertially focused stream of target cells back to the input.[31]

In this paper, we present a simple microfluidic sample preparation method using a spiral microchannel device, resulting in enhanced detection of virus from blood samples using unbiased metagenomic sequencing. To our best knowledge, this is the first time to demonstrate a whole workflow from microfluidic sample preparation to metagenomic sequencing-based virus detection. Our spiral inertial microfluidic device is operated in a recirculatory regime so that virus can be isolated via negative selection from the diluted blood while large host cells are kept in the recirculating flow. Conventionally, it has been considered difficult to isolate small particles like viruses (a few tens or hundreds of nanometers) with an inertial microfluidic device because these small particles are prone to Brownian motion and are too small to be inertially focused with the net lift force in a microchannel.[32] We separate viruses from the host cells —red blood cells (RBC), white blood cells (WBC), and platelets—by keeping the host cells (larger than or equal to 3 μm in diameter) focused in the closed-loop while collecting the outer-wall output which mainly consists of free-floating viruses in background fluid, along with cell-free nucleic acid. In this manner, negatively selected viral particles can be collected with the buffer solution, with most of host cells depleted in an automated and fully contained manner (Fig. 1 A). The utility of spiral microfluidics with negative selection scheme was verified by processing whole blood samples spiked with cytomegalovirus (CMV), analyzing the resulting suspension with quantitative PCR and viral sequencing, and comparing the results between treated and untreated samples. We observed significant increase in the number of viral reads as well as viral genome coverage depth for microfluidics-treated samples. The increase in viral reads was higher in samples with low virus concentration, which suggests potential for using our device and operation scheme for pre-treatment of clinical whole blood samples.

Experimental Section

Device fabrication

The spiral inertial microfluidic device was fabricated with polydimethysiloxane (PDMS) following standard soft-lithographic microfabrication techniques as descried previously.[31] The master mold with specific microchannel dimensions was designed with AutoCAD software and then fabricated with micro-milling machine (Whits Technologies, Singapore) on aluminum. PDMS replica was fabricated by casting degassed PDMS (10:1 mixture of base and curing agent of Sylgard 184, Dow corning Inc.) onto the aluminum mold, curing on the hot plate for 10 minutes at 150 degrees and peeling the cured PDMS off the mold. Holes for fluidic access were punched with disposable biopsy punches (Integra™ Miltex®). The punched PDMS replica was then irreversibly bonded to a silicone film (BISCO HT-6240 40 Duro silicone sheet, 0.25mm-thick, Rogers Corp.) placed on a glass slide after treating both surfaces with plasma machine (Femto Science, Korea). The assembled device was placed in a 60 degrees oven for 1 hour to stabilize the bonding further.

Sample preparation

Fresh human whole blood samples collected in an ethylenediaminetetraacetic acid (EDTA) vacutainer (purple top) were purchased from Research Blood Components, LLC (Boston, MA, USA) and spiked with known concentrations of cytomegalovirus (ATCC-2011–8) to generate samples representing a range of clinically-relevant viral loads (10^4-10^8 CMV copies/mL whole blood). Plasma samples were prepared by centrifugation of whole blood for 10 minutes at 994 RCF, followed by collection of the plasma layer. As a control, some plasma samples underwent lysis of cell and viral membranes by combining 200 μL of plasma samples with 800 μL of buffer AVL (Qiagen).

In preparation for loading in the spiral microfluidic device, samples were diluted in buffer comprised of phosphate-buffered saline without calcium and magnesium (PBS, Corning®) plus 0.1% w.t. bovine serum albumin (BSA, Sigma-Aldrich) to prevent non-specific binding of cells and viral particles to device surface and tubing. Whole blood samples were diluted 100-fold (100 uL whole blood in 9,900 uL buffer) and plasma samples were diluted 10-fold (1 mL plasma in 9 mL buffer). Due to differences in the number of host cells, different dilution factors were chosen for whole blood and plasma samples to yield the best rejection ratio of host cells (Supplementary Fig. 1).

Experimental setup for closed-loop operation of spiral microfluidic device (“C-sep”)

Closed-loop operation of spiral inertial microfluidic device was done by connecting a peristaltic pump (Cole-Parmer) to the device with silicone tubing (Masterflex platinum-cured tubing, L/S 14, Cole-Parmer) with sample tubes (Falcon® Polystyrene Sterile Centrifuge Tubes, Corning®) loaded on a rack (Fig. 1 B). Tubing connected to the inner-wall side outlet was fed back to the input tube for closed-loop operation while the output sample was being collected at the outer-wall side outlet tubing. This operation was continued until all input volume was processed with the optimized flow rate of 1.6 mL/min (Fig. S1).

Immunofluorescence staining and flow cytometer analysis

All input and output samples were aliquoted in a volume of 100 μL and stained with 10 μL of allophycocyanin (APC)-conjugated mouse antihuman CD41a reagent (Miltenyi Biotec) for 30 minutes at 4 degrees in the dark. The stained samples were then analyzed by BD Accuri C6 flow cytometer (BD Bioscience) to quantify the number of RBC/WBCs/platelets in each sample based on the number of events gated by fluorescence intensity, forward-scattering and side-scattering, accordingly. To evaluate how much cell was removed from the input to the output, we recorded the volume of each input and output sample and multiplied these volumes by the number of events per processed sample volume in the aliquoted samples to calculate the total number of each cell type.

Extraction and quantification of viral nucleic acid with quantitative polymerase chain reaction (qPCR)

Nucleic acid was extracted using the MagMax Pathogen RNA/DNA kit (ThermoFisher) per the manufacturer's instructions. Nucleic acid was extracted from between 100μL-1mL of sample, depending on sample type and microfluidic processing.

CMV total nucleic acid was quantified by qPCR using *Power* SYBR® Green RNA-to-C_T™ (Applied Biosystems). Samples were assayed in triplicate with a total reaction volume of 10 μL, including 3 μL of template and 0.3 μL of each primer per the manufacturer's instructions. Thermocycling conditions were: 95 degrees for 10 minutes, followed by 45 cycles of 95 degrees for 15 seconds and 60 degrees for 60 seconds. Primer sequences were after Peres *et al.*[33]: Forward=GAAGGTGCAGGTGCCCTG, Reverse=GTSTCGACGAACGACGTACG. Viral copies were calculated by comparison to a standard curve generated using a custom synthesized DNA fragment (gBlocks®, IDT) quantified by NanoDrop (ThermoFisher Scientific). Final concentrations were adjusted for differences in sample volumes and dilutions during processing.

Viral next-generation sequencing (NGS)

Sequencing libraries were prepared from 1ng of extracted nucleic acid using the Nextera XT DNA library preparation kit (Illumina), as previously described[9]. Sequencing libraries were quantified in triplicate using the KAPA Library Quantification kit (KAPA Biosystems) according to manufacturer's instructions. Samples were pooled at equal molarity and sequenced on the Illumina MiSeq platform using paired-end 100bp reads.

Reads were demultiplexed, and initial taxonomic assignment was performed using Kraken[34]. Using viral-ngs[35], reads were cleaned of human reads, filtered against a reference genome corresponding to the HHV5 strain Merlin (NC_006273.2), and underwent *de novo* assembly of the CMV genome with refinement by scaffolding against the same reference genome. To compare CMV genome coverage between samples, 450,000 reads were randomly selected for each sample to ensure comparability, and then CMV reads were aligned to the reference genome (NC_006273.2) in BWA using the following parameters -k 12 -B 2 -O 3; duplicate reads were excluded.

Results & Discussion

Evaluation of Spiral Microfluidic Device Performance

Particles or cells of different sizes experience different magnitude of inertial and drag forces in a spiral microchannel and equilibrate at different lateral positions. Since the net lift force on a particle suspended in a plane Poiseuille flow is proportional to particle diameter (a_p) to the power of 4 $\left(\sim a_p^4\right)$ ($F_L = \rho G^2 C_L a_p^4$, where ρ is the density of fluid medium, G is the shear rate of the fluid given by $G = U_{max}/D_h$, U_{max} is the maximum fluid velocity, D_h is the microchannel hydraulic diameter, and C_L is the lift coefficient which is a function of the particle position across the channel cross-section and channel Reynolds number (Re)) and the Dean drag force on a particle is proportional to particle diameter ($\sim a_p$) ($F_D = 3\pi\mu U_{dean} a_p = 5.4\times10^{-4}\pi\mu De^{1.63} ap$, where De (Dean number) is given by $De = \frac{\rho U_f D_h}{\mu}\sqrt{\frac{D_h}{2R}}$. U_f is average velocity of fluid, μ is dynamic viscosity of fluid, and R is radius of curvature of curved microchannel.)[23], larger particles or cells are more dominated by inertial lift force than Dean drag and tend to be equilibrated at inner side of the spiral microchannel during operation. On the other hand, smaller particles are more dominated by Dean drag and tend to be dispersed throughout the microchannel, following two counter-rotating vortices known as Dean vortices in the spiral microchannel. Spiral microchannel is carefully designed to have trapezoidal cross-section of 800 μm width, 70 and 40 μm height at inner-wall and outer-wall side, respectively, to focus relatively large host cells (RBC/WBC/Platelets, ≥3 μm in diameter) while relatively small virus particles are spread throughout the microchannel, as depicted in Fig. 1 A. Host cells are located near the inner-wall (IW) side of the microchannel when they reach the bifurcation point at the outlet and are fed back to the input tube during recirculation of spiral microfluidic device while virus particles are negatively selected and constantly collected at the outer-wall (OW) outlet. A trapezoidal cross-section was chosen to allow more space for the inner-wall focused host cells [30] so that the focusing behavior is maintained until the end of closed-loop operation when the concentration of the solution becomes higher. The inertially focused streamline of host cells at the inner-wall is further assisted by the ZweifachFung effect[36,37] due to the smaller fluidic resistance, thus the flow rate is higher at the innerwall outlet. As can be seen in Fig. 1 C and D, the fluid collected at the OW outlet looked clear due to the depletion of host cells. This process takes place in an automated and fully contained manner, which can be compatible with biosafety requirements for processing known or unknown viral pathogens from clinical samples.

To evaluate the separation efficiency, we processed both whole blood and plasma samples. Figure 2 A illustrates the separation efficiency of our spiral microfluidic device operated in a closed-loop manner. For whole blood samples (n=9), the total number of RBC and WBC was reduced by 98% (from 6.7× ^{7} ××$10^8$7 to 1.5×10^7 cells) and the number of platelets was reduced by 36% (from 2.6 10 to 1.7 10 cells). For plasma samples (n=9), which should not contain RBC or WBCs but do contain residual platelets, the total number of platelets was reduced by 69% (from 2.4×10^8 to 7.4×10^7 cells). Depletion of platelets in the whole blood samples was found to be less effective than in the plasma samples because steric particle crowding effects became more severe for the whole blood samples and affected particle focusing behavior towards the end of C-sep. when host cell concentration was highly

increased.[24] The recovery of CMV nucleic acid was measured by qPCR, from samples before and after microfluidic processing (Fig. 2 B). These results demonstrate successful recovery of CMV from both whole blood and plasma across a range of viral concentrations. Overall recovery was calculated from the slope of data points and estimated to be 114.1% for whole blood samples and 103.5% for plasma samples. Estimated recovery greater than 100% could have come from sampling error, or the inexact nature of qPCR.

Assessment of virus genome recovery by metagenomic sequencing

We initially performed metagenomic sequencing from whole blood, plasma, and lysed plasma from a sample with high viral load (10^8 CMV copies/mL of whole blood) before and after microfluidic separation. The lysed plasma sample was used as a control in which host cells and virus are lysed prior to microfluidic separation; we expected that host nucleic acid would not be depleted by inertial microfluidics. To assess recovery of sequencing reads from CMV compared to host, we first performed metagenomic classification of all reads using Kraken.[34] This showed an increase in CMV reads and a decrease in human reads for both whole blood and plasma but not lysed plasma (Fig. 3A). CMV reads increased from 2.0% to 4.0% for the microfluidics-treated whole blood sample and from 9.0% to 17.0% for the microfluidics-treated plasma sample, while CMV reads decreased from 2.0% to 0.8% for the microfluidic-streated lysed plasma sample, which may reflect sampling variability. Reads that were not classified as CMV or human generally belonged to microbial species that we commonly observe in our sequencing negative controls, representing background from water or sequencing reagents. We also assembled full CMV genomes and found an increase in the depth of coverage of the CMV genome by approximately 2 fold after microfluidic processing of both whole blood and plasma, normalizing for differences in total sequencing depth (Fig. 3B). Depth increased for MF-treated samples by 2.1 fold for whole blood (from 12 to 25) and by 1.8 fold for plasma (from 75 to 133), while coverage depth did not increase for lysed plasma sample.

The utility of spiral microfluidics for viral sequence enrichment was even greater at lower, clinically relevant viral loads (10^4 and 10^6 CMV copies/mL whole blood), levels at which full CMV genomes could not be assembled with the depth of sequencing used for the present study. To compare recovery of CMV reads before and after microfluidic processing, we aligned all reads to the CMV reference genome and calculated the number of unique mapped CMV reads per sample. We observed a consistent increase in CMV reads after microfluidics, which was more pronounced in whole blood than plasma and at lower viral loads. Specifically, mapped viral reads increased after microfluidic processing by 16.5, 3.3 and 2.1 fold for whole blood samples and by 6.3, 2.0 and 1.9 fold for plasma samples with 10^4, 10^6 and 10^8 CMV copies/mL, respectively (Fig. 3C and 3D). Furthermore, this increase in the number of CMV reads was evenly distributed across the full length of the CMV genome for both plasma and whole blood (Fig. 3E). We do not observe evidence of a greater increase in the read depth for certain regions of the CMV genome (Fig. 3E), indicating that microfluidics processing does not introduce biases in viral recovery. Overall, these results suggest that our spiral microfluidic platform enhances viral detection especially in samples where host background is higher and/or viral content is low, as is the case for many clinical samples.

Conclusion

We developed a sample preparation platform using a spiral microfluidic device that can isolate virus from host cells in whole blood or plasma in an automated, fully-contained manner. Removal of host cells through size-based spiral inertial microfluidic sorting with recirculation led to the reduction of human (host) background reads in metagenomic sequencing for viral detection and sequencing. Further studies are needed to assess recovery of intact infectious virus for other downstream processes. We anticipate that our device can help ease the sample preparation process and improve the sensitivity of sequencing-based viral detection for viral clinical samples by enabling direct use of whole blood samples for WGS sample preparation as well as eliminating the need for centrifuge or membrane-based filters.

Supplementary Material

Refer to Web version on PubMed Central for supplementary material.

Acknowledgement

This work was supported by a generous Broad*next*10 gift from the Broad Institute, NIH R01 (R01AI117043), and NIH U24 Sample Sparing assay program (U24-AI118656).

Reference

(1). Ngoi CN; Siqueira J; Li L; Deng X; Mugo P; Graham SM; Price MA; Sanders EJ; Delwart EJ Gen. Virol 2016, 97, 3359–3367.

(2). Wilson MR; Zimmermann LL; Crawford ED; Sample HA; Soni PR; Baker AN; Khan LM; DeRisi JL Am. J. Transplant 2017, 17, 803–808. [PubMed: 27647685]

(3). Grard G; Fair JN; Lee D; Slikas E; Steffen I; Muyembe J-J; Sittler T; Veeraraghavan N; Ruby JG; Wang C; Makuwa M; Mulembakani P; Tesh RB; Mazet J; Rimoin AW; Taylor T; Schneider BS; Simmons G; Delwart E; Wolfe ND; Chiu CY; Leroy EM PLoS Pathog. 2012, 8, e1002924. [PubMed: 23028323]

(4). McMullan LK; Folk SM; Kelly AJ; MacNeil A; Goldsmith CS; Metcalfe MG; Batten BC; Albariño CG; Zaki SR; Rollin PE; Nicholson WL; Nichol ST N. Engl. J. Med 2012, 367, 834–841. [PubMed: 22931317]

(5). Kosoy OI; Lambert AJ; Hawkinson DJ; Pastula DM; Goldsmith CS; Hunt DC; Staples JE Emerg. Infect. Dis 2015, 21, 760–764. [PubMed: 25899080]

(6). Stremlau MH; Andersen KG; Folarin OA; Grove JN; Odia I; Ehiane PE; Omoniwa O; Omoregie O; Jiang P-P; Yozwiak NL; Matranga CB; Yang X; Gire SK; Winnicki S; Tariyal R; Schaffner SF; Okokhere PO; Okogbenin S; Akpede GO; Asogun DA; Agbonlahor DE; Walker PJ; Tesh RB; Levin JZ; Garry RF; Sabeti PC; Happi CT PLoS Negl. Trop. Dis 2015, 9, e0003631. [PubMed: 25781465]

(7). Gire SK; Goba A; Andersen KG; Sealfon RSG; Park DJ; Kanneh L; Jalloh S; Momoh M; Fullah M; Dudas G; Wohl S; Moses LM; Yozwiak NL; Winnicki S; Matranga CB; Malboeuf CM; Qu J; Gladden AD; Schaffner SF; Yang X; Jiang P-P; Nekoui M; Colubri A; Coomber MR; Fonnie M; Moigboi A; Gbakie M; Kamara FK; Tucker V; Konuwa E; Saffa S; Sellu J; Jalloh AA; Kovoma A; Koninga J; Mustapha I; Kargbo K; Foday M; Yillah M; Kanneh F; Robert W; Massally JLB; Chapman SB; Bochicchio J; Murphy C; Nusbaum C; Young S; Birren BW; Grant DS; Scheiffelin JS; Lander ES; Happi C; Gevao SM; Gnirke A; Rambaut A; Garry RF; Khan SH; Sabeti PC Science 2014, 345, 1369–1372. [PubMed: 25214632]

(8). Park DJ; Dudas G; Wohl S; Goba A; Whitmer SLM; Andersen KG; Sealfon RS; Ladner JT; Kugelman JR; Matranga CB; Winnicki SM; Qu J; Gire SK; Gladden-Young A; Jalloh S;

Nosamiefan D; Yozwiak NL; Moses LM; Jiang P-P; Lin AE; Schaffner SF; Bird B; Towner J; Mamoh M; Gbakie M; Kanneh L; Kargbo D; Massally JLB; Kamara FK; Konuwa E; Sellu J; Jalloh AA; Mustapha I; Foday M; Yillah M; Erickson BR; Sealy T; Blau D; Paddock C; Brault A; Amman B; Basile J; Bearden S; Belser J; Bergeron E; Campbell S; Chakrabarti A; Dodd K; Flint M; Gibbons A; Goodman C; Klena J; McMullan L; Morgan L; Russell B; Salzer J; Sanchez A; Wang D; Jungreis I; Tomkins-Tinch C; Kislyuk A; Lin MF; Chapman S; MacInnis B; Matthews A; Bochicchio J; Hensley LE; Kuhn JH; Nusbaum C; Schieffelin JS; Birren BW; Forget M; Nichol ST; Palacios GF; Ndiaye D; Happi C; Gevao SM; Vandi MA; Kargbo B; Holmes EC; Bedford T; Gnirke A; Ströher U; Rambaut A; Garry RF; Sabeti PC Cell 2015, 161, 1516–1526. [PubMed: 26091036]

(9). Matranga CB; Andersen KG; Winnicki S; Busby M; Gladden AD; Tewhey R; Stremlau M; Berlin A; Gire SK; England E; Moses LM; Mikkelsen TS; Odia I; Ehiane PE; Folarin O; Goba A; Kahn SH; Grant DS; Honko A; Hensley L; Happi C; Garry RF; Malboeuf CM; Birren BW; Gnirke A; Levin JZ; Sabeti PC Genome Biol. 2014, 15, 519. [PubMed: 25403361]

(10). Gu W; Crawford ED; O'Donovan BD; Wilson MR; Chow ED; Retallack H; DeRisi JL Genome Biol. 2016, 17, 41. [PubMed: 26944702]

(11). Rios M; Daniel S; Chancey C; Hewlett IK; Stramer SL Clin. Infect. Dis. 2007, 45, 181–186. [PubMed: 17578776]

(12). Lustig Y; Mannasse B; Koren R; Katz-Likvornik S; Hindiyeh M; Mandelboim M; Dovrat S; Sofer D; Mendelson E J. Clin. Microbiol 2016, 54, 2294–2297. [PubMed: 27335150]

(13). Shim JS; Ahn CH; Beaucage G; Nevin JH; Lee J-B; Puntambekar A; Lee JY; Liu C; Gould J; Hood L; Heath JR Lab Chip 2012, 12, 863. [PubMed: 22277985]

(14). Lee KK; Ahn CH; Schmitt J; Nevin JH; Lee J-B; Puntambekar A; Lee JY; Lilja H; Laurell T; Hood L; Heath JR Lab Chip 2013, 13, 3261. [PubMed: 23793507]

(15). Zhang X-B; Wu Z-Q; Wang K; Zhu J; Xu J-J; Xia X-H; Chen H-Y Anal. Chem 2012, 84, 3780–3786. [PubMed: 22449121]

(16). Dimov IK; Basabe-Desmonts L; Garcia-Cordero JL; Ross BM; Ricco AJ; Lee LP; Kwong GA; Liu C-C; Gould J; Hood L; Heath JR; Balis UJ; Tompkins RG; Haber DA; Toner M Lab Chip 2011, 11, 845–850. [PubMed: 21152509]

(17). CHEN X; CUI D; LIU C; LI H Sensors Actuators B Chem. 2008, 130, 216–221.

(18). Vandelinder V; Groisman A Anal. Chem 2006, 78, 3765–3771. [PubMed: 16737235]

(19). Tachi T; Kaji N; Tokeshi M; Baba Y Anal. Chem 2009, 81, 3194–3198. [PubMed: 19364145]

(20). Haeberle S; Brenner T; Zengerle R; Ducrée J Lab Chip 2006, 6, 776–781. [PubMed: 16738730]

(21). Gorkin R; Park J; Siegrist J; Amasia M; Lee BS; Park J-M; Kim J; Kim H; Madou M; Cho Y-K; Ouellette M; Bergeron MG; Ducrée J Lab Chip 2010, 10, 1758. [PubMed: 20512178]

(22). Liu C; Mauk M; Gross R; Bushman FD; Edelstein PH; Collman RG; Bau HH Anal. Chem 2013, 85, 10463–10470. [PubMed: 24099566]

(23). Wang SQ; Sarenac D; Chen MH; Huang SH; Giguel FF; Kuritzkes DR; Demirci U Int. J. Nanomedicine 2012, 7, 5019–5028. [PubMed: 23055720]

(24). Di Carlo D; Irimia D; Tompkins RG; Toner M Proc. Natl. Acad. Sci. U. S. A 2007, 104, 18892–18897. [PubMed: 18025477]

(25). Bhagat AAS; Kuntaegowdanahalli SS; Papautsky I Microfluid. Nanofluidics 2009, 7, 217–226.

(26). Di Carlo D Lab Chip 2009, 9, 3038–3046. [PubMed: 19823716]

(27). Warkiani ME; Khoo BL; Wu L; Tay AKP; Bhagat AAS; Han J; Lim CT Nat. Protoc 2015, 11, 134–148. [PubMed: 26678083]

(28). Warkiani ME; Tay AKP; Guan G; Han J Sci. Rep 2015, 5, 11018. [PubMed: 26154774]

(29). Warkiani ME; Wu L; Tay AKP; Han J Annu. Rev. Biomed. Eng 2015, 17, 1–34. [PubMed: 26194427]

(30). Rafeie M; Zhang J; Asadnia M; Li W; Warkiani ME; Ni Z; Ni Z; Han J; Han J; Lim CT Lab Chip 2016, 16, 2791–2802. [PubMed: 27377196]

(31). Ryu H; Choi K; Qu Y; Kwon T; Lee JS; Han J Anal. Chem 2017, 89, 5549–5556. [PubMed: 28402103]

(32). Salafi T; Zeming KK; Zhang Y Lab Chip 2017, 17, 11–33.

(33). Peres RMB; Costa CRC; Andrade PD; Bonon SHA; Albuquerque DM; de Oliveira C; Vigorito AC; Aranha FJP; de Souza CA; Costa SC B. BMC Infect. Dis 2010, 10, 147.

(34). Wood DE; Salzberg SL Genome Biol. 2014, 15, R46. [PubMed: 24580807]

(35). Metsky HC; Matranga CB; Wohl S; Schaffner SF; Freije CA; Winnicki SM; West K; Qu J; Baniecki ML; Gladden-Young A; Lin AE; Tomkins-Tinch CH; Ye SH; Park DJ; Luo CY; Barnes KG; Shah RR; Chak B; Barbosa-Lima G; Delatorre E; Vieira YR; Paul LM; Tan AL; Barcellona CM; Porcelli MC; Vasquez C; Cannons AC; Cone MR; Hogan KN; Kopp EW; Anzinger JJ; Garcia KF; Parham LA; Ramírez RMG; Montoya MCM; Rojas DP; Brown CM; Hennigan S; Sabina B; Scotland S; Gangavarapu K; Grubaugh ND; Oliveira G; Robles-Sikisaka R; Rambaut A; Gehrke L; Smole S; Halloran ME; Villar L; Mattar S; Lorenzana I; Cerbino-Neto J; Valim C; Degrave W; Bozza PT; Gnirke A; Andersen KG; Isern S; Michael SF; Bozza FA; Souza TML; Bosch I; Yozwiak NL; MacInnis BL; Sabeti PC Nature 2017, 546, 411–415. [PubMed: 28538734]

(36). Svanes K; Zweifach BW Microvasc. Res 1968, 1, 210–220.

(37). Fung Y-C Microvasc. Res 1973, 5, 34–48. [PubMed: 4684755]

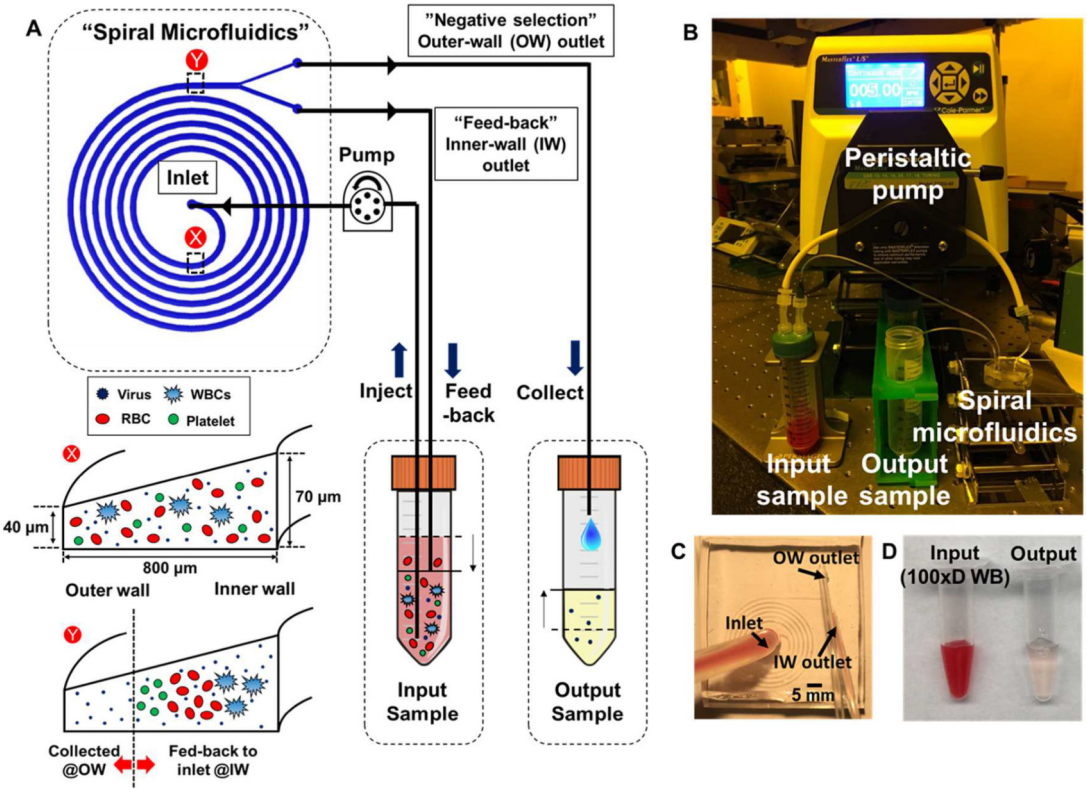

Figure 1.

(A) Schematic of closed-loop separation ("C-sep") spiral microfluidic device platform with negative selection scheme (B) Photograph of experimental setup (C) Magnified view of spiral microfluidic device (D) Comparison between input (100 times diluted whole blood) and microfluidics (MF)-treated samples

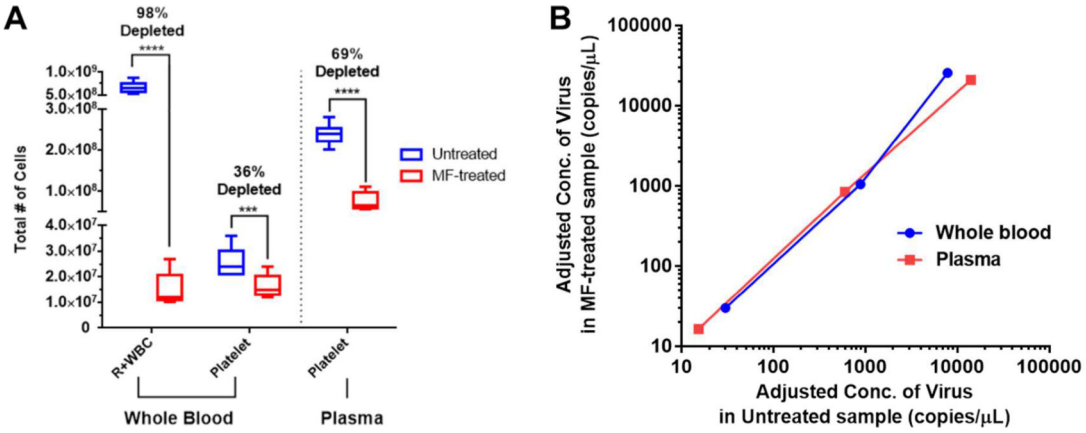

Figure 2.

(A) Total number of cells (calculated from flow cytometry results) in untreated and MF-treated samples for whole blood and plasma samples. Each bar is drawn with data points of 9 samples. (B) Concentration of CMV (viral copies/uL) recovered as output from MF (yaxis) versus input (x-axis).

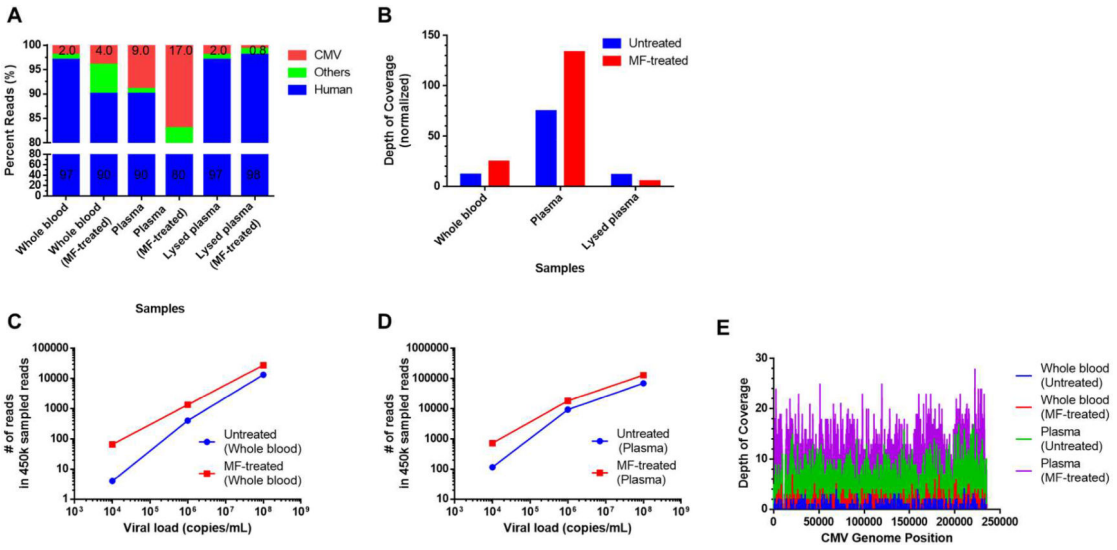

Figure 3.

(A) Metagenomic classification of sequencing reads by Kraken for samples derived from whole blood spiked with 10^8 CMV copies/mL. (B) Normalized coverage depth of CMV whole genome assemblies for samples in (A). (C) Comparison of CMV reads before (untreated) and after (MF-treated) microfluidic treatment of whole blood samples spiked with a range of CMV viral loads (10^4, 10^6, 10^8 copies/mL whole blood). (D) Comparison of CMV reads before (untreated) and after (MF-treated) microfluidic treatment of plasma samples (E) Plot showing the depth of coverage (y-axis) across the CMV genome (x-axis) in samples derived from whole blood spiked with 10^6 CMV copies/mL. Depth of coverage is the number of sequenced reads that aligned to the CMV genome at each base pair position from 450,000 sampled reads.